JOURNAL OF SPACECRAFT AND ROCKETS
Vol. 34, No. 3, May–June 1997

Moon–Sun Attitude Sensor

Daniele Mortari
University of Rome "La Sapienza," Rome 00138, Italy

The basic ideas and the preliminary feasibility study of an experimental sensor for spacecraft attitude determination are presented. This instrument, based on a low-cost charge-coupled-device camera, is a moon tracker that records its images in the visible spectrum. The subsequent image processing enables this sensor to provide redundant data for attitude determination. Up to six different directions and two angles could actually be evaluated. The moon orbit and magnitude, the instrument operability, and the data reduction, as well as the attitude determination, have been briefly analyzed. The sensor cost is expected to be low, and its accuracy would increase with the complexity of the moon image processing software.

Nomenclature

$\boldsymbol{A}$	= attitude matrix ($\boldsymbol{Av} = \boldsymbol{s}$)
M	= magnitude
$\boldsymbol{R}[\boldsymbol{v}, \vartheta]$	= 3×3 matrix performing the rigid rotation about the $\boldsymbol{v}$ direction of the ϑ angle
r_e, r_m	= Earth and moon radii, respectively
$\boldsymbol{S}, \boldsymbol{s}$	= vector and unit vector defined in the spacecraft reference system, respectively
$\boldsymbol{V}, \boldsymbol{v}$	= vector and unit vector defined in the inertial reference system, respectively
$\boldsymbol{x}, \boldsymbol{y}$	= camera reference system axes
ϑ	= phase angle
ξ	= angle between the moon-to-spacecraft and the moon-to-sun directions
φ_m, ω_m	= true anomaly and perigee argument of the moon orbit, respectively
Ω_m, i_m	= right ascension of the ascending node and inclination of the moon orbit, respectively

Subscripts

c	= spacecraft
e	= Earth
k	= moon spin axis
m	= moon
s	= sun
δ	= symmetry axis of the moon's illuminated area (directed toward the sun side)

Introduction

As far as attitude determination is concerned, only the wide-field-of-view (FOV) star trackers can be used in a stand-alone configuration because they are the only existing attitude sensors that provide more than one direction. In fact, to determine a three-axis attitude, at least two directions are needed. If only one direction is available, the orientation of the spacecraft (S/C) about this direction would remain undetermined by an unknown phase angle ϑ. Limitations in the use of star trackers arise from both their very high costs and the large memory required for the stars pattern recognition process. Hence, if other attitude sensors are chosen, at least two different sensors are needed for estimating the attitude. A new attitude sensor, called the moon–sun sensor, capable of being used in a stand-alone configuration and of expected low cost is proposed.

The derivation that led to the proposed sensor is based on two facts. 1) The moon is a gravity-stabilized satellite and, therefore, it shows, approximately, always the same side to an Earth-orbiting S/C. This implies that a moon reference image (MRI), such as those shown in Figs. 1 and 2, is available in the inertial reference system (IRS) as a function of time and of the S/C, sun, and moon orbital positions. 2) By comparing the MRI with the moon observed image (MOI) and by a proper image processing of the MOI, it is possible to derive useful information for attitude determination.

In fact, from the image processing of the MOI it is possible to identify in the spacecraft reference system (SRS) 1) the S/C-to-moon direction $\boldsymbol{s}_{cm}$, defined as the direction pointing to the center of the circle of minimum radius containing the illuminated area (Fig. 3), 2) the symmetry axis $\boldsymbol{s}_\delta$ of the moon illuminated area ($\boldsymbol{s}_\delta$ and $\boldsymbol{s}_{cm}$ also identify the plane where the sun, moon, and S/C lie), 3) the angle ξ between the moon-to-sun and the moon-to-S/C directions (this angle can be evaluated in three different ways: from the observed moon magnitude and the S/C–moon distance, from the observed shape of the sun terminator in the moon, and by the orbit ephemeris), and 4) the moon-to-sun direction $\boldsymbol{s}_{ms}$ derived from ξ, $\boldsymbol{s}_{cm}$, and $\boldsymbol{s}_\delta$. By comparing the MRI with the MOI, it is also possible to evaluate 1) the phase angle ϑ by a shifting technique, which rotates the MRI over the MOI about the moon's center until the matching is, in the least-square terms, at its best; 2) the moon spin axis $\boldsymbol{s}_k$ using the same shifting technique; and 3) the two directions $\boldsymbol{s}_1$ and $\boldsymbol{s}_2$ of the principal momentum of inertia of the moon illuminated area.

The S/C attitude estimation can then be performed either by applying one of the existing algorithms to the $\boldsymbol{s}_{cm}$, $\boldsymbol{s}_\delta$, $\boldsymbol{s}_{ms}$, $\boldsymbol{s}_k$, $\boldsymbol{s}_1$, and $\boldsymbol{s}_2$ unit vectors or by applying Eq. (12) (to be given), which simply uses only the S/C-to-moon direction $\boldsymbol{s}_{cm}$ and the phase angle ϑ.

Daniele Mortari is an assistant professor of the Aerospace Engineering School of the University of Rome "La Sapienza" of Rome, Italy. He received a degree in Nuclear Engineering, attended the Aerospace Engineering School, and was trained at NASA Goddard Space Flight Center in Attitude and Orbit Control Systems. He joined the San Marco Project and cooperated in the activities for the San Marco 5 spacecraft. As a researcher, he developed several new algorithms for attitude determination, attitude dynamics and control, misalignment determination, stars pattern recognition, matrix eigenanalysis, and data processing. He is the author of more than 30 papers. He is a member of the American Astronautical Society. E-mail: daniele@crarisc1.psm.uniroma1.it.

Received July 29, 1996; presented as Paper 96-3618 at the AIAA/AAS Astrodynamics Specialists Conference, San Diego, CA, July 29–31, 1996; revision received Jan. 15, 1997; accepted for publication Jan. 22, 1997.

Fig. 1 Full moon.

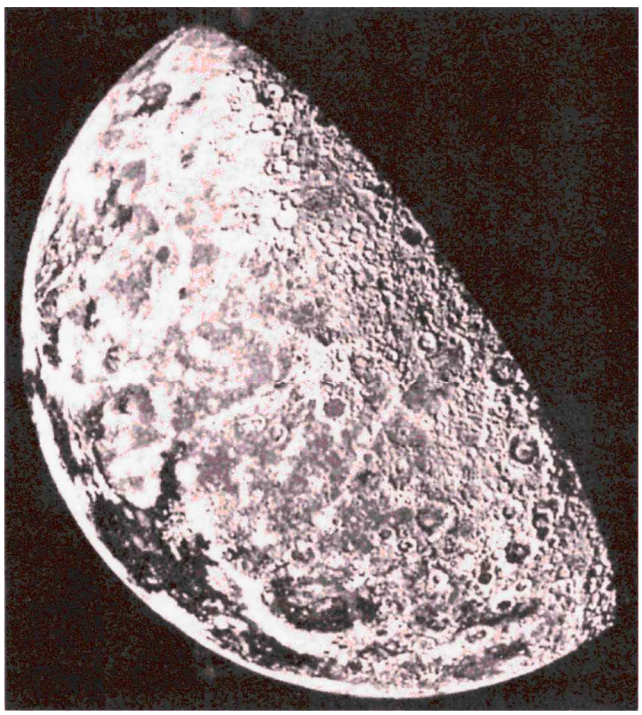

Fig. 2 Moon observed with $\xi = 75$ deg.

Instrument Description and Mode of Operation

The moon–sun attitude sensor is expected to be a low-cost conventional charge-coupled-device (CCD) camera that tracks the moon and records its images in the visible spectrum. The images could be provided by means of a camera that outputs a matrix of pixels, each representing a gray tone. The camera signal threshold (which establishes the maximum value of the measured radiance at which the minimum of the gray tone scale is assigned to a pixel) should be based on the emission value, in the visible spectrum, of the new moon (moon not illuminated).

The operational phases of this instrument could be considered as the following: 1) the acquisition/identification stage, during which the sensor looks for the moon by scanning a region of the sky until the moon is captured within the instrument FOV (the moon is identified as such if the observed moon magnitude falls within the moon magnitude range) and 2) the tracking stage, the nominal operational

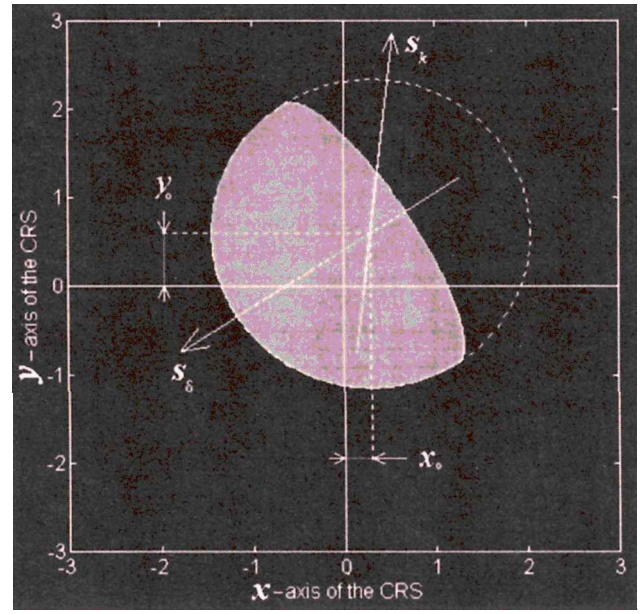

Fig. 3 Moon as observed by the camera.

mode, when the instrument constantly tracks the moon while its images are being processed.

As a function of the S/C–moon distance, the moon appears, in the SRS, as a circle with radius ranging from 0.2336 to 0.2912 deg. For a three-axis-stabilized S/C, the camera FOV should be designed according to the maximum relative moon motion, which occurs during the longest Earth obscuration time. This occurs to the highest altitude S/C orbiting on the moon orbital plane. During the Earth obscuration period, for a 36,000-km S/C, the moon direction appears displaced by 2.65 deg, while for a 500-km S/C, it appears displaced by 2.25 deg. Therefore, with the constraint of having the moon centered at ($x_o = 0$, $y_o = 0$), the camera FOV should be at least twice the moon direction displacement angle, that is, $2 \times 2.65 = 5.3$ deg. Should this FOV imply too small a pixel size to keep a good image resolution, it would be possible to decrease it to a compromised value, provided that during the Earth obscuration period, the moon tracking is based on predictions derived from the previous relative moon motion in the camera reference system. In the following paragraphs, the moon orbit and magnitude, the instrument operability, the data reduction, and the attitude determination will be briefly analyzed.

Moon Orbit

Inasmuch as the moon's mass (7.355×10^{22} kg) cannot be disregarded with respect to the Earth's mass (5.98×10^{24} kg), a Keplerian orbit model does not describe the motion of the moon sufficiently well. A simplified orbit model can be based on the three-body theory to take into account the sun's gravitational effects. The special perturbation and the general perturbation models (some of which involve up to 1600 periodical terms) are more accurate. It is also possible to have expressions derived by a best fit of the measured data. One of these expressions, American Ephemeris,[1] which is presented next, describes the moon mean motion:

$$\begin{aligned}
\varphi_m &= 270.434164 + 13.1763965268t \\
&\quad - 8.5 \times 10^{-13}t^2 + 3.9 \times 10^{-20}t^3 \\
\omega_m &= 334.329356 + 0.1114040803t \\
&\quad - 7.739 \times 10^{-12}t^2 - 2.6 \times 10^{-19}t^3 \\
\Omega_m &= 259.183275 - 0.0529539222t \\
&\quad + 1.557 \times 10^{-12}t^2 + 5 \times 10^{-20}t^3 \\
i_m &= 5.145396374
\end{aligned} \tag{1}$$

where t is the time difference (in days) between the time at which the computation is required and the reference time (Jan. 1, 1900, at 12:00; Julian date = 2415010). This model has been adopted, as well as the following moon orbit data: moon–Earth average distance of 384,400 km, orbital average period of 27.31661 days, eccentricity ranging from 0.044 to 0.067 (average, 0.054900489), orbit inclination with respect to the ecliptic plane ranging from 4°58′ to 5°19′ (average, 5°8′43″), period of the right ascension of the ascending node derivative of 18.6 years, period of the perigee argument derivative of 8.85 years, equatorial plane inclined by 6°41′ and 1°32′30″ with respect to orbital and ecliptic planes, respectively, and, finally, the moon radius of 1738 km. Furthermore, the sun–Earth distance range is $1.47\times10^8 \div 1.5\times10^8$ km (average, 1.4959965×10^8 km = 1 AU).

Instrument Operability

With the exception of magnetometers (the practical use of which is limited to altitudes less than 1000 km) and Earth horizon sensors, all other sensors are subjected to an eclipse period. A conventional system using, for instance, an Earth horizon sensor and a solar sensor cannot control the S/C attitude when the sun is hidden by the Earth, nor can a moon–sun-based system maintain control when the moon is not visible (the moon and the sun have approximately the same probability of being visible by a S/C). Thus, what really matters is the percentage of operational control time with respect to the orbit period.

The moon–sun sensor operability is inhibited in three orbital circumstances: 1) when the moon cannot be observed because it is hidden by the Earth, 2) in the rare cases of moon eclipses (the next moon eclipses will occur at 03:59–07:21 March 24, 1997, as partial; 18:08–21:24 Sept. 16, 1997, as total; and 11:22–13:44 July 28, 1999, as partial), and 3) when the sun falls into the sensor FOV. To avoid this last event, which coincides also with the case that the moon is not illuminated, a sun presence sensor should command the instrument shutter closed.

Cases 1 and 2 can easily be predicted by moon, S/C, and sun orbit positions. The moon obscuration or the moon eclipse, which are both identified by the same equation, occur when

$$\boldsymbol{V}_m^T\boldsymbol{V} < r_e^2 - \sqrt{\left(\boldsymbol{V}_m^T\boldsymbol{V}_m - r_e^2\right)\left(\boldsymbol{V}^T\boldsymbol{V} - r_e^2\right)} \tag{2}$$

where $\boldsymbol{V} = \boldsymbol{V}_c$ for the moon obscuration and $\boldsymbol{V} = \boldsymbol{V}_s$ for the moon eclipse.

If ϑ_{FOV} is the camera FOV, then case 3 occurs when

$$\boldsymbol{v}_{mc}^T\boldsymbol{v}_{sc} > \cos\vartheta_{\text{FOV}} \tag{3}$$

The moon visibility timetable is derived from the moon's relative motion in the body coordinate system. This timetable provides insight into the tracking system control law, which is actually determined by the moon image motion as detected and measured by the tracking camera.

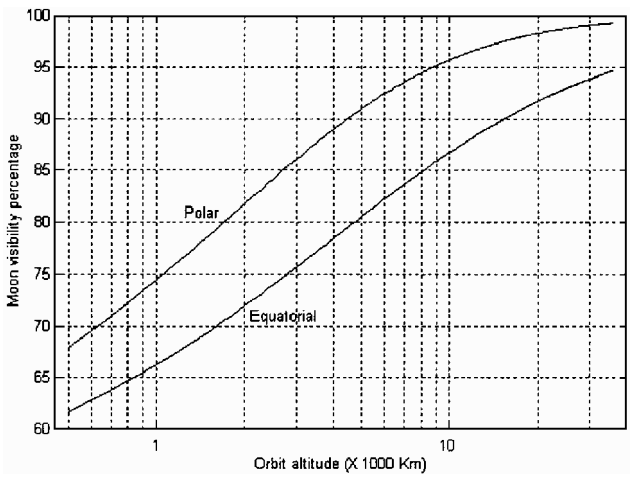

Fig. 4 Moon visibility.

Table 1 Phase law table

ξ	$P(\xi)$	ξ	$P(\xi)$	ξ	$P(\xi)$
0	1.000	50	0.288	110	0.041
5	0.929	60	0.225	120	0.027
10	0.809	70	0.172	130	0.017
20	0.625	80	0.127	140	0.009
30	0.483	90	0.089	150	0.004
40	0.377	100	0.061	160	0.001

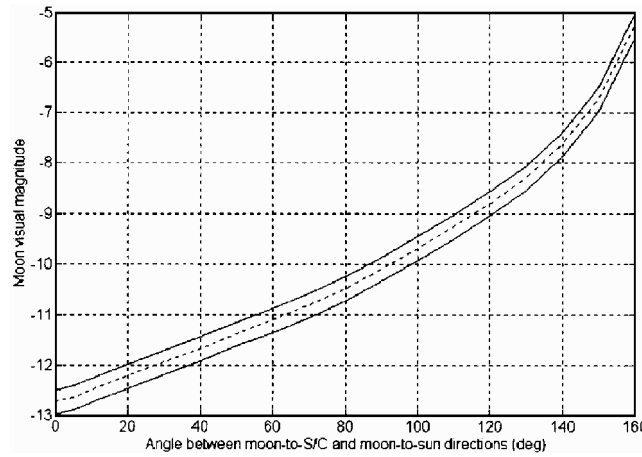

Fig. 5 Moon magnitude range.

Figure 4 shows the moon visibility percentage (moon not obscured by the Earth) as a function of the S/C altitude, ranging from 500 km up to 36,000 km, and for two extreme cases of circular orbits lying on the moon's orbital plane (equatorial) or perpendicular to it (polar).

Moon Magnitude

The moon visual magnitude M depends mainly on two parameters: the distance $|\boldsymbol{V}_{cm}|$ between the S/C and the moon and the angle ξ between the moon-to-sun and moon-to-S/C directions. The function $M(|\boldsymbol{V}_{cm}|, \xi)$ has been provided by introducing the phase law $P(\xi)$, experimentally derived,[1] and given by Table 1.

If $|\boldsymbol{V}_{cm}|$ is expressed in astronomical units, the moon visual magnitude $M(|\boldsymbol{V}_{cm}|, \xi)$ is given by

$$M(|\boldsymbol{V}_{cm}|, \xi) = 0.23 + 5\log_{10}(|\boldsymbol{V}_{cm}|) - 2.5\log_{10}[P(\xi)] \tag{4}$$

Figure 5 shows the behavior of the moon magnitude as a function of the angle ξ for the Earth–moon average distance $|\boldsymbol{V}_m| =$ 384,400 km (the dotted line) and for the two S/C–moon limit distances, $|\boldsymbol{V}_{cm}|_{\min} =$ 342,021.9 km and $|\boldsymbol{V}_{cm}|_{\max} =$ 426,242.5 km, of a S/C orbiting at 36,000 km in the orbit plane of the moon. As shown, the moon magnitude falls within the range from −13 to −5. The visual magnitudes of the other bright objects are $M_{\text{sun}} = -26.7$, $M_{\text{venus}} = -4.4$ (at its maximum), and $M_{\text{sirius}} = -1.5$ (brightest star). Therefore, with the exception of very rare and momentary events (i.e., the 1906 supernova, which appeared with magnitude −9.5), no bright objects fall within the moon magnitude range. Hence, the measured moon magnitude can be used to identify the moon during the acquisition phase.

Attitude Data in the IRS

Based on the orbital ephemeris, it is possible to evaluate the S/C, moon, and sun positions, that is, the $\boldsymbol{V}_c$, $\boldsymbol{V}_m$, and $\boldsymbol{V}_s$ vectors, at a given time and defined in the IRS. The S/C-to-moon and the moon-to-sun vectors are simply given as $\boldsymbol{V}_{cm} = \boldsymbol{V}_m - \boldsymbol{V}_c$ and $\boldsymbol{V}_{ms} = \boldsymbol{V}_s - \boldsymbol{V}_m$, respectively, whereas the corresponding unit vectors are

$$\boldsymbol{v}_{cm} = \frac{\boldsymbol{V}_{cm}}{\sqrt{\boldsymbol{V}_{cm}^T\boldsymbol{V}_{cm}}} \qquad \boldsymbol{v}_{ms} = \frac{\boldsymbol{V}_{ms}}{\sqrt{\boldsymbol{V}_{ms}^T\boldsymbol{V}_{ms}}} \tag{5}$$

The angle ξ, between $\boldsymbol{v}_{mc}(=-\boldsymbol{v}_{cm})$ and $\boldsymbol{v}_{ms}$, is given by

$$\xi = \cos^{-1}\left(-\boldsymbol{v}_{ms}^T \boldsymbol{v}_{cm}\right) \tag{6}$$

and the symmetry axis of the moon illuminated area $\boldsymbol{v}_\delta$ (perpendicular to $\boldsymbol{v}_{mc}$, toward the sun side) is

$$\boldsymbol{v}_\delta = (\boldsymbol{v}_{ms} + \boldsymbol{v}_{cm}\cos\xi)/\sin\xi \tag{7}$$

The moon's spin axis $\boldsymbol{v}_k$, whose direction can be considered approximately fixed in space, is inclined $1°32'30''$ with respect to the Earth's spin axis, whereas its longitude, derived from the moon's latitudinal libration motion, is provided by available software. It is, however, convenient (the reasons will be clarified in the next section) to evaluate the unit vector $\boldsymbol{v}_k$ as perfectly perpendicular to $\boldsymbol{v}_{cm}$.

Based on the S/C, moon, and sun orbital positions, as well as on the moon attitude (to take into account both the moon latitudinal and longitudinal librations), it is possible to obtain in the IRS the image of the moon as seen from the S/C. This moon image generator (MIG) can be implemented with a given range of sophistication, depending on the attitude accuracy requirements. This range would span from the simplest MIG model, which would produce only the edge of the moon illuminated area (moon illuminated horizon plus sun terminator), through an intermediate more detailed one, which could additionally consider some surface features (i.e., some large craters edges), up to the most sophisticated image, which would be obtained, similarly to virtual reality images, by including also the shadows of the known features of the viewed moon surface. The better the MRI is, the more it will resemble the observed one; the difference would be that the MRI would appear rotated by a phase angle ϑ with respect to the MOI. In this case the MRI, like the MOI, is available as a pixels matrix of gray tones. It is then possible to assign a weight value to each pixel, for instance, proportional to its gray tone. The MRI can then be regarded as a two-dimensional mass body and, therefore, its two principal inertia axes $\boldsymbol{v}_1$ and $\boldsymbol{v}_2$ can be evaluated.

Attitude Data in the SRS

Let us consider the moon image as detected by the tracking camera shown in Fig. 3. By processing the moon image, the theory of which is not dealt with in this paper, it is possible to identify the coordinates (x_o, y_o) of the minimum-radius circle of the lunar horizon (from which the direction $\boldsymbol{s}_{cm}$ is easily derived), as well as the image symmetry axis $\boldsymbol{s}_\delta$ of the moon illuminated area ($\boldsymbol{s}_\delta$ is perpendicular to $\boldsymbol{s}_{cm}$ and directed toward the sun side). These data could be computed, for instance, by an easy image processing scheme that considers all of the nonblack pixels as white. Thus, the symmetry axis becomes a figure's inertia principal axis, whereas the coordinates (x_o, y_o) could be derived as follows: 1) by measuring, in the MRI, the distance of the figure's center of gravity from the moon's center and transposing this distance, in the MOI, along the symmetry axis and 2) by the evaluation, in the MOI, of the center of the circle of minimum radius containing the illuminated area (i.e., by applying a best fitting technique).

The angle ξ could be derived in three different ways using 1) the orbit ephemeris and Eq. (6), 2) the observed moon magnitude M, and 3) a best fitting technique of the expected sun terminator equation with the observed sun terminator. Method 2 leads to the definition of the function $\xi(M, |\boldsymbol{V}_{cm}|)$ that can be obtained, for instance, by applying a best fitting technique (using either the simple or the Legendre orthogonal polynomials) to the data (M, ξ), provided in Table 1 and Eq. (4), for the given S/C–moon distance $|\boldsymbol{V}_{cm}|$. Because Eq. (4) amplifies, by the term $\log_{10}[P(\xi)]$, the small errors at the highest value of ξ, a high polynomial degree is needed (to keep the precision). This implies, unfortunately, a loss of precision due to a quasisingular matrix inversion. Therefore, particular attention must be given to the best fitting technique used. Based on performed trials, the collapsed axis method best fitting technique (Annex A of Ref. 2), which compresses the ξ axis, with a six-degree polynomial is suggested. Method 3 requires evaluation of the sun terminator equation, which is the equation of a projected ellipse.

Once both $\boldsymbol{s}_{cm}$ and $\boldsymbol{s}_\delta$ have been evaluated, the moon-to-sun direction is provided by

$$\boldsymbol{s}_{ms} = -\boldsymbol{R}[\boldsymbol{s}_\delta \times \boldsymbol{s}_{cm}, \xi]\,\boldsymbol{s}_{cm} \tag{8}$$

where

$$\boldsymbol{R}[\boldsymbol{n}, \xi] = \boldsymbol{I}\cos\xi + (1-\cos\xi)\boldsymbol{n}\boldsymbol{n}^T + \tilde{\boldsymbol{n}}\sin\xi \tag{9}$$

represents the 3×3 matrix performing the rigid rotation about the unit vector $\boldsymbol{n} = \boldsymbol{s}_\delta \times \boldsymbol{s}_{cm}$ of the ξ angle.

The two principal inertia axes of the moon illuminated area, $\boldsymbol{s}_1$ and $\boldsymbol{s}_2$, are evaluated by considering each pixel of the MOI as having a mass proportional to its gray tone.

The evaluation of the phase angle ϑ can be obtained by shifting the MRI over the MOI until the overlapping images match the best, that is, when a least-square difference between them is at a minimum. The best condition for the phase angle determination would occur when the moon appears as fully illuminated (Fig. 1), whereas the ξ angle is roughly determined. Exactly the opposite occurs when the bright moon portion becomes small. This quite good compensation effect allows the attitude estimation accuracy to be almost independent of the moon lighting values, that is, of the whole ξ angle range. As shown by comparison between Figs. 1 and 2, the smaller ξ becomes (that is, when the illuminated area increases), the more the contrast of the moon image decreases; this represents another good compensation effect. The phase angle ϑ could also be computed by fitting the observed sun terminator with its equation.

The identification of the moon spin axis $\boldsymbol{s}_k$ can be done only after evaluation of the phase angle ϑ. Once this angle has been computed, then the unknown $\boldsymbol{s}_k$ unit vector is provided by

$$\boldsymbol{s}_k = \boldsymbol{R}[\boldsymbol{v}_{cm}, \vartheta]\boldsymbol{v}_k \tag{10}$$

Attitude Determination

S/C attitude can be optimally estimated by using one of the existing algorithms[3–6] with the observed directions $\boldsymbol{s}_{cm}, \boldsymbol{s}_{ms}, \boldsymbol{s}_\delta, \boldsymbol{s}_k, \boldsymbol{s}_1$, and $\boldsymbol{s}_2$.

The condition for the highest accuracy in three-axis attitude determination is that of having orthogonal measured directions. While a typical 16-deg FOV star tracker would provide (in the best case) observed directions separated by 16 deg, the moon–sun sensor (in the worst case of having only the two unit vectors $\boldsymbol{s}_{cm}$ and $\boldsymbol{s}_\delta$) would provide orthogonal directions, that is, the best accuracy condition. Moreover, in this case, the attitude matrix can be evaluated using the original nonoptimal TRIAD algorithm[3] by the simple formula

$$\boldsymbol{A} = [\boldsymbol{s}_{cm}\ \boldsymbol{s}_\delta\ (\boldsymbol{s}_{cm} \times \boldsymbol{s}_\delta)][\boldsymbol{v}_{cm}\ \boldsymbol{v}_\delta\ (\boldsymbol{v}_{cm} \times \boldsymbol{v}_\delta)]^T \tag{11}$$

where the $\boldsymbol{s}_\delta$ unit vector can be replaced by one of the $\boldsymbol{s}_1, \boldsymbol{s}_2$, and $\boldsymbol{s}_k$ directions.

It is also possible to evaluate the attitude matrix by using the $\boldsymbol{s}_{cm}$ unit vector together with the phase angle ϑ. The attitude matrix can then be computed as the product of two rigid rotations as follows:

$$\boldsymbol{A} = \boldsymbol{R}[\boldsymbol{s}_{cm}, \vartheta]\,\boldsymbol{R}\left[\frac{\boldsymbol{v}_{cm} \times \boldsymbol{s}_{cm}}{|\boldsymbol{v}_{cm} \times \boldsymbol{s}_{cm}|}, \cos^{-1}\left(\boldsymbol{v}_{cm}^T \boldsymbol{s}_{cm}\right)\right] \tag{12}$$

where the first rotation, performed about the direction of $\boldsymbol{v}_{cm} \times \boldsymbol{s}_{cm}$, brings $\boldsymbol{v}_{cm}$ to be coincident with $\boldsymbol{s}_{cm}$, whereas the second rotation is performed about $\boldsymbol{s}_{cm}$ by the phase angle ϑ.

Conclusions

The basic ideas as well as a preliminary feasibility study of a new attitude sensor, which tracks the moon and records its images in the visible spectrum, have been presented. By means of the moon image processing, this instrument would provide redundant data for attitude determination. The moon orbit and magnitude, the instrument operability, the data reduction, and the attitude determination have been briefly described. The two main features making this proposed type of instrument rather interesting are 1) its capability to be used

in a stand-alone configuration for S/C attitude determination and 2) its expected low cost.

Whereas a low-cost attitude system, composed of an infrared Earth horizon sensor and a sun sensor, provides only the S/C-to-Earth and the S/C-to-sun directions (that is, two unit vectors, which is also the minimum data basis for three-axis attitude determination), the moon–sun sensor would provide 1) the S/C-to-moon direction, 2) the symmetry axis direction of the moon illuminated area, 3) the angle between the moon-to-S/C and moon-to-sun directions, 4) the moon-to-sun direction, 5) the phase angle, 6) the moon spin axis, and 7) the two directions of the principal momentum of inertia of the moon illuminated area. This is four additional unit vectors and two angles in the attitude data basis.

The cost is expected to be low for two main reasons. 1) Because the attitude data provided by the moon–sun sensor are derived from the analysis of the moon illuminated area (which involves a high number of pixels), it is possible to adopt a pixel size much greater than that of CCD star tracker. 2) The influence of temperature variations on the CCD camera performance should be, for the given moon magnitude range [−13 to −5], much lower than that of CCD star trackers and, therefore, an expensive thermal control system would be avoided. Hence, for these reasons, the moon–sun sensor image-digitalizing camera could be a conventional low-cost CCD camera. The cost would increase as the accuracy requirement increases because higher precision would imply more sophisticated software (i.e., a more detailed MIG and/or software able to recognize craters edges/shapes and so on). Therefore, the sensor cost would be dependent on the software complexity. This means that, in the case of a very sophisticated software, most of the cost would be in building the sensor prototype; once the software has been developed and tested, it can be used for all of the moon–sun sensors. Most of the cost of wide-FOV star trackers is for hardware; every unit has approximately the same high cost.

From the accuracy point of view, it is expected that the moon–sun sensor would provide good/high precision. The pixel size of a conventional CCD camera is much greater than that of CCD star tracker and, therefore, provides a lower local precision, but the resulting final precision of the sensor has to be thought of as integrated over the large illuminated area of the moon. Therefore, as with the cost, the precision of this sensor would depend on the MIG and the MOI processing software and not on its hardware. Even though the moon–sun sensor would provide accuracy lower than that supplied by star trackers, there are a lot of planned S/C with budget limitations much more stringent than their attitude precision requirements.

In conclusion, the properties of this sensor should make it quite suitable when money allocation for attitude sensors is limited but a three-axis attitude estimation is required.

Acknowledgments

This work has been supported by the Italian Space Agency under Contract RS82. I should like to warmly thank Carlo Massini (Aerotech World Trade Corporation) because the main idea that led to this paper came in discussions with him while commuting to and from work. I also would like to thank Paolo Campanelli and Bruno Bernabei (Italian Air Force), Julie Deutschmann (NASA Goddard Space Flight Center), and Carlo Arduini (University of Rome) for support and advice provided.

References

[1]Rowe, J. N., "Modeling the Positions of the Sun, Moon, and Planets," *Spacecraft Attitude Determination and Control*, edited by J. R. Wertz, 1st ed., Vol. 73, D. Reidel, Dordrecht, The Netherlands, 1973, pp. 138–143, 823.

[2]Mortari, D., and Arduini, C., "Attitude Dynamics Induced by the Thermal Transition on a Spin Stabilized Cable Boom System," *Advances in the Astronautical Sciences*, Vol. 87, Pt. 1, 1994, pp. 53–66.

[3]Shuster, M. D., and Oh, S. D., "Three-Axis Attitude Determination from Vector Observations," *Journal of Guidance and Control*, Vol. 4, No. 1, 1981, pp. 70–77.

[4]Mortari, D., "Energy Approach Algorithm for Attitude Determination from Vector Observations," AAS/AIAA 5th Annual Space Flight Mechanics Meeting, Paper 95-207, Albuquerque, NM, Feb. 1995; also *Advances in the Astronautical Sciences* (to be published).

[5]Mortari, D., "EULER-2 and EULER-*n* Algorithms for Attitude Determination from Vector Observations," International Federation of Automatic Control, Conf. on Intelligent Autonomous Control in Aerospace, Paper T2-9, Beijing, PRC, Aug. 1995.

[6]Mortari, D., "EULER-q Algorithm for Attitude Determination from Vector Observations," *Advances in the Astronautical Sciences*, Vol. 93, Pt. 2, 1996, pp. 1009–1020.

A. C. Tribble
Associate Editor